# Mode Conversion of Ultrafast Pulses by Grating Structures in Layered Dielectric Waveguides

Tao Liang and Richard W. Ziolkowski, *Fellow, IEEE*

***Abstract*— Various grating configurations are introduced to develop structures for the mode conversion of an ultrafast, ultrawide-bandwidth optical pulse propagating in a layered dielectric waveguide. Introducing a new technique for efficient, real-time mode extraction, we examine these schemes with a full-wave, vector, finite difference time domain (FDTD) Maxwell equation simulator. The resulting FDTD simulator is very flexible and accurate; it is capable of modeling the interaction of few- or many-cycle optical pulsed modes with finite, aperiodic gratings with complex material configurations. The grating structure can be tailored to the pulsed optical modes of interest with this FDTD simulator. It is used to design a composite mode-conversion grating structure that realizes a 29.45% increase in the converted mode energy for an ultrafast six-cycle optical pulse over that achieved with standard uniform grating convertors.**

***Index Terms*—Dielectric waveguides, FDTD, mode conversion, mode extraction, numerical modeling, ultrafast optical pulses.**

## I. Introduction

With the development of techniques for generating ultrafast laser pulses and the increasingly apparent potential for their applications, there is a corresponding need to understand the interaction between such ultrawide-bandwidth optical pulses and advanced materials and devices. In this paper we develop further the time domain numerical modeling tools that can be used to simulate mode conversion of optical pulsed modes by grating structures in planar dielectric waveguides. Our desire to model such grating structures, particularly with ultrafast pulse interactions, stems from the recognition, for example, that optical communication systems are being driven to shorter pulse regimes to increase the available information bandwidths. Devices will then need to be designed for these ultrafast pulses to meet traditional needs. For instance, one designs a dielectric waveguide so that the major portion of the propagating energy of its fundamental mode resides in its core region. To attenuate or measure the power in this waveguide mode, one common approach is to convert it into a higher order mode with a grating so that the propagating energy will be re-distributed from the core into the cladding region. The amount of attenuation or measured power can be adjusted by selectively designing the amount of absorption in the cladding material. While most of these issues are well understood for single frequency operation, traditional designs prove to be inefficient for ultrawide-bandwidth, ultrafast pulsed modes. The grating structure must be tailored to the frequency content in the pulsed guided mode.

The design on gratings in single frequency applications is well established. Among these applications are the electromagnetic diffraction and scattering problems under plane wave incidence [1], and the guidance problems for electromagnetic mode propagation in waveguides [2], [3]. Mode conversion is achieved in the latter when the propagation constants of the modes of interest satisfy an appropriate phase matching condition. A number of methods, both analytical and numerical, have been proposed to analyze these grating structures for single frequency excitation. Most of them treat the gratings as periodic structures of infinite extent with reasonably homogeneous, nondispersive materials in each unit cell. However, the ultrafast pulse environment will require aperiodic finite grating structures in the presence of dispersive materials that can be effective over a few optical cycles which corresponds to a large frequency content. Fabrication technologies for wavelength-sized structures of this type are currently available in several formats and are being improved constantly. However, few modeling approaches can handle finite, aperiodic structures in complex material environments.

The modeling of optical pulse propagation in complex media has generally been accomplished with one-dimensional, scalar models (see, for example, [4]). These traditional models have become extremely complex, but are attractive since they quickly provide reasonable explanations for a variety of observed phenomena. However, they are inadequate as the wavelength approaches the device size. The beam propagation method (see, for example, [5]–[8]) has become a very popular numerical method for numerical modeling optical beam propagation in complex media and waveguides. However, without many of the recent corrective augumentations, these beam propagation method (BPM) algorithms are inaccurate for highly reflective, polarization dependent materials and structures. Many of these analytical and numerical approaches also assume that the pulses are constructed around a carrier frequency and extremely narrow bandwidth envelopes. They are traditionally analyzed in linear media with Fourier analysis and stepped-frequency techniques. In linear media gratings can then be designed by adopting an optimization approach on the basis of the Fourier spectrum of the pulses. Yet with the large number of parameters to be optimized, such as grating periods, grating modulation depths, and material properties, as well as

Manuscript received October 15, 1996. This work was supported in part by the Office of Naval Research under Grant N0014-95-1-0636 and by the Air Force Office of Scientific Research, Air Force Materiel Command, USAF, under Grant F49620-96-1-0039.

The authors are with the Electromagnetics Laboratory, Department of Electrical and Computer Engineering, University of Arizona, Tucson, AZ 85721 USA.

Publisher Item Identifier S 0733-8724(97)06660-7.

different grating configurations, such an optimization becomes very complicated and cumbersome to achieve.

It is thus desirable to have a simple and efficient way to provide some insight into the behavior of grating structures interacting with ultrafast optical pulses. The finite-difference time-domain method (FDTD) is a very good choice for these simulations. First introduced by Yee [9], this discrete numerical method directly solves the full-wave vector Maxwell's equations in differential form. It has become a very popular method in the microwave regime and has been used recently to model ultrafast optical pulse propagation in linear and nonlinear media [10], [11] and to model the interactions with linear and nonlinear interfaces [12] and gratings [13]–[15]. It provides an extremely flexible simulation environment that can model arbitrary geometries and material distributions, including dispersion and nonlinearities. It can handle pulses consisting of one cycle or thousands.

To understand quantitatively the mode conversion process for ultrafast optical pulses, we have developed an efficient real-time mode extraction technique for use with our FDTD simulator. This augmented FDTD simulator has enabled us to carry out a thorough investigation of various grating structures that could be used to mode convert ultrafast optical pulses. These include periodic and aperiodic rectangular and sinusoidal gratings whose unit-cell lengths are adjusted coarsely or finely. We have found that the aperiodic gratings with coarse adjustments in the unit cell lengths that are designed to convert different frequency components in the pulsed modes at different times and locations within the grating structure are the most efficient.

In Section II, we present the FDTD numerical simulator used to describe the interaction of ultrafast pulsed modes with finite, aperiodic grating structures. In Section III, we describe the technique we have developed to extract the desired mode information from these numerical FDTD results. Several cases with uniform gratings are presented to validate our approach. In Section IV, various composite grating structure designs are explored and their efficiency in converting pulsed optical waveguide modes are characterized. It will be shown that an aperiodic mode-conversion grating structure can be designed that results in a 29.45% increase in the converted mode energy for an ultrafast six-cycle optical pulsed mode over that achieved with standard uniform grating convertors.

## II. Numerical Simulator

Because of its ability to model complex structures and materials as well as single or many cycle pulses, the finite difference time domain approach to solving Maxwell's equations [10] was selected for the present mode conversion investigation. The associated geometric, material, and source flexibilities makes the FDTD simulator the method of choice for our problems. In FDTD simulations Maxwell's equations are solved to second-order accuracy by replacing the differential relations by centered finite differences, both in space and in time. The electric and magnetic field components reside on a staggered grid (the components of the electric and magnetic fields and the material properties are interleaved in a precise manner on the grid) and the resulting update equations for these field components are integrated forward in time in a leapfrog fashion. For all of the simulations to be presented below, the regions of interest were discretized into square cells whose sides were 1/30 of the free space wavelength defined by the carrier frequency of the source. The corresponding FDTD time step size is restricted to insure numerical stability; it was taken to be the two-dimensional (2-D) Courant value [10].

The basic structure for our investigations, hereafter referred to as the basis waveguide, was a two dimensional dielectric slab waveguide supporting TE modes. The direction of propagation was taken to be along the $z$-axis; the infinite direction was taken along the $y$-axis. Thus the components of a TE mode were $E_y$, $H_x$, and $H_z$; and the material discontinuites representing the waveguide boundaries were along the $x$-axis. The basis waveguide consists of three layers and is surrounded by free space. The center layer is the core region and has a dielectric constant of 2.25. The upper and lower layers are the cladding regions and have a dielectric constant of 2.03. All of these layers are taken to be 1.0 $\mu$m thick.

The possible modes of the basis waveguide are calculated with a standard frequency domain technique [16]. For the carrier frequency of $3 \times 10^{14}$ Hz, the basis waveguide can support seven propagating modes, denoted by mode 1 through mode 7. To initiate a certain mode, the known transverse mode field distribution [16] is multiplied by the desired time excitation. The excitation signal is an envelope of choice times a sinusoidal wave at the carrier frequency. For the simulations to be presented below, the selected signal results in a six-cycle pulse containing two smooth turn-on cycles, two unit sinusoidal cycles, and two smooth turn-off cycles. It is referred to as the 2-2-2 pulse. Fig. 1 shows its spectrum. For the simulation cases treated below this 2-2-2 pulse spectrum has most of its frequency content above the cutoffs of the first seven propagating modes. This 2-2-2 pulsed mode is launched into the simulation region from a total field/scattered field boundary [10]. The fields are followed throughout the entire simulation region as they evolve in time.

The mode conversion is realized by a grating structure which is constructed by deforming the boundaries between the core region and the cladding regions in either a rectangular or a sinusoidal profile. The sinusoidal profile is approximated in a stair-stepped fashion; this representation is very good approximation with the specified spatial discretization. The various rectangular gratings we have considered are illustrated in Fig. 2.

It is well known [2] that for a monochromatic excitation, the grating period in a mode conversion grating is dictated by a phase matching condition. To convert from the $i$th waveguide mode with the propagation constant $\beta_i$ to the $j$th waveguide mode with the propagation constant $\beta_j$, this phase matching condition requires the grating period $\Lambda$ to satisfy the relation

$$\Lambda = \frac{2\pi}{|\beta_i - \beta_j|}. \tag{1}$$

The grating periods for the mode conversion between mode 1 and mode 5 in the basis waveguide that are associated with various frequencies contained in the 2-2-2 excitation pulse are

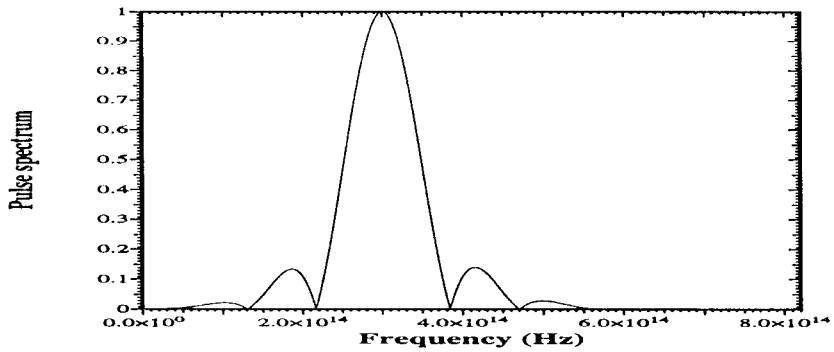


Fig. 1. Spectrum of the 2-2-2 pulse.

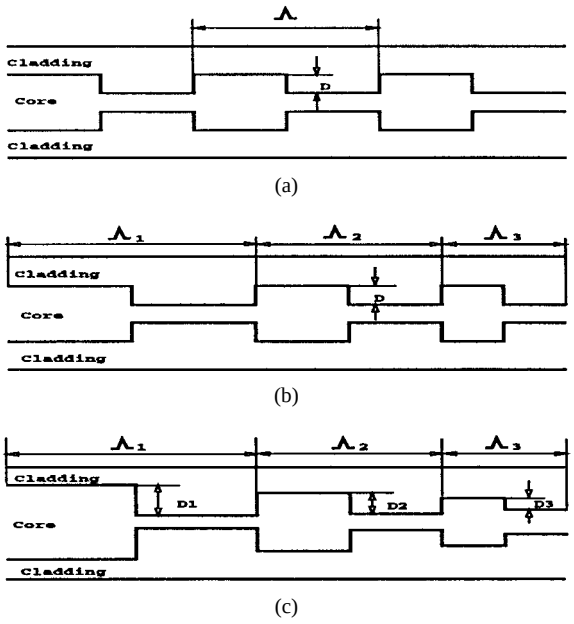


Fig. 2. Finite rectangular grating structures investigated. (a) Uniform, (b) frequency chirped, and (c) frequency chirped and depth modulated.

listed in Table I. These grating periods are specified in terms of the number of FDTD cells required to model them in the simulation region.

## III. Pulsed Mode Extraction

The FDTD approach gives the complete description of the time evolution of the fields. However, we are interested primarily in how much energy exists in any one waveguide mode. A mode is strictly a frequency domain concept; the pulsed waveguide field is merely a composite structure consisting of a single or multiple waveguide modes excited with different frequencies. Thus the total energy in one mode will be a superposition of all of the single frequency energies in that mode excited by the source. To quantify the degree to which one pulsed mode is converted into another pulsed mode, we have augmented the basic FDTD simulator with the following pulsed mode extraction scheme. It is a straightforward generalization of the standard monochromatic method which uses mode orthogonality to decompose a given guided wave into each of its modal components so that one can quantify how much energy is in a specified mode for a single frequency of excitation.

TABLE I
Grating Periods in Terms of the Number of FDTD Grid Cells for Conversion from Mode 1 to Mode 5 at the Indicated Frequencies

| frequency($10^{14}$ Hz) | 2.5 | 2.8 | 3.0 | 3.2 | 3.5 |
|---|---|---|---|---|---|
| grating period(# of cells) | 114 | 122 | 126 | 131 | 136 |

Let $e_i(x)$ be the transverse field distribution of the $i$th TE mode. The total electric field in the waveguide $E_y(x,z,t)$ is a superposition of all possible modes, namely

$$E_y(x,z,t) = \sum_i V_i(z,t)e_i(x) + E_y^{\text{radiation}}(x,z,t). \quad (2)$$

The mode amplitude factor $V_i(z,t)$ contains complete information about the longitudinal distribution of the electric field as a function of the time. All of the radiation mode effects have been lumped together in the term $E_y^{\text{radiation}}$. Since the radiation and guided modes are orthogonal and since the simulation is excited initially with a propagating mode, very little energy will be found in any of the radiation modes until some discontinuity such as the grating structure is encountered. Even then, since the waveguide itself is only weakly modulated by the grating structure, most of the energy of interest remains in the propagating modes.

Just as it does in the frequency domain, mode orthogonality allows us to extract all the desired time domain mode information from the fields. This includes the energy present in a specified mode of interest. In particular, we take the transverse mode distribution $e_i(x)$ at the carrier frequency. With mode orthogonality

$$\int_{-\infty}^{\infty} e_i(x)e_j(x)\,dx = 0 \quad (3)$$

and normalization of the mode distribution

$$\int_{-\infty}^{\infty} e_i^2(x)\,dx = 1 \quad (4)$$

the mode amplitude factor $V_i(z,t)$ is obtained via projection of the field $E_y$ onto the $i$th mode as

$$V_i(z,t) = \int_{-\infty}^{\infty} E_y(x,z,t)e_i(x)\,dx. \quad (5)$$

Note that this mode amplitude factor is also the equivalent voltage for the $i$th mode. The equivalent current for the $i$th

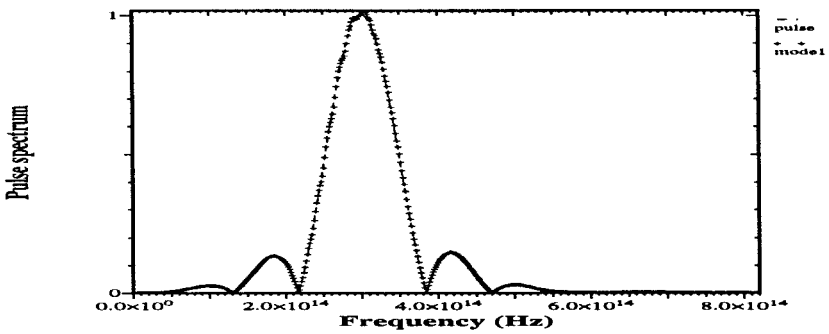


Fig. 3. Spectrum of extracted mode 1.

mode is obtained in a similar manner from the transverse component of the magnetic field

$$I_i(z,t) = \int_{-\infty}^{\infty} H_x(x,z,t) h_i(x)\, dx \tag{6}$$

where $h_i(x)$ is the normalized transverse magnetic field mode distribution. Therefore, the energy $\mathcal{E}_i$ in the $i$th mode passing through a plane $z = const$ is given by

$$\mathcal{E}_i(z) = \int_{-\infty}^{\infty} V_i(z,t) I_i(z,t)\, dt \tag{7}$$

The orthogonality of the transverse mode distributions thus allows us to determine in time the mode amplitude factors at any longitudinal location. This result also reflects the way the initial signal is excited, which is given by first specifying a spatial transverse mode distribution and then multiplying it by a certain time envelope. Thus by using the FDTD simulator to obtain the electric and magnetic fields in any specified $z = const$ plane, we can calculate the energy in a mode directly by this transverse mode projection algorithm.

This mode extraction approach is also very efficient since it avoids the complexity of invoking any Fourier analysis for the pulsed signal. It is implemented directly in the FDTD as follows:

$$V_i(k\Delta z, n\Delta t) = \sum_m E_y(k\Delta z, n\Delta t) e_i(m\Delta x)\Delta x \tag{8}$$

$$I_i(k\Delta z, n\Delta t) = \sum_m H_x(k\Delta z, n\Delta t) h_i(m\Delta x)\Delta x \tag{9}$$

$$\mathcal{E}_i(k\Delta z) = \sum_n V_i(k\Delta z, n\Delta t) I_i(k\Delta z, n\Delta t)\Delta t \tag{10}$$

where $m = 1, \cdots, M$ and $M\Delta x$ is the transverse dimension of the simulation region; and $n = 1, \cdots, N$ where $N$ is the number of times steps taken in the simulation. Both $E_y$ and $H_x$ are directly available from the FDTD simulation. Therefore, our approach is a real-time extraction technique.

Reference [17] discussed an analogous technique for mode extraction from FDTD field information. That approach obtained the coefficients of all the guided modes by the method of least squares which requires the inversion of a matrix system. For mode conversion, we are interested in only a few specific modes, typically the original mode and the converted mode. The associated mode amplitude factors can be extracted through (5) and (6) more efficiently by directly invoking the mode orthogonality property, without the additional computational cost required for matrix inversion. This can be done at each computational step with little overhead and provides additional information including the rate at which the mode conversion is proceeding. Furthermore, from the strict function approximation perspective (Best Approximation Theorem [18]), the projection from the total field onto the propagating modes is indeed in the least square sense, since mode orthogonality holds for all modes, including the guided modes and radiation modes.

To validate the FDTD mode extraction technique, we initiated a combination of mode 1 and mode 5 with the 2-2-2 pulse envelope into the simulation region. At a distance $118\lambda_0$ away from the source plane, the mode amplitude factor for each mode was extracted. The energy in mode 1 and mode 5 were found to be 97.64 and 97.03% of their initial energy. The small decrease in the energy was found to be due to the fact that the FDTD method will excite some nonpropagating reactive field energy in the vicinity of the source plane. Moreover, some of the low frequency content of the spectrum is below the cutoff frequency for these modes so it is attenuated immediately. Taking separate measurements of the mode energies along the waveguide outside of this aperture region showed that the energy in each mode was well defined and well maintained once the mode became established.

We also note that if desired, mode information at any frequency is immediately available by Fourier transforming the extracted mode amplitude factors into the frequency domain. As shown in Figs. 3 and 4, the spectrum of the extracted mode amplitude factor for each mode is in close agreement with that of the original 2-2-2 pulse excitation (shown as a dashed line). These results demonstrate that the information about each individual frequency component within the pulsed mode spectrum is correctly extracted with our mode extraction technique. The slight differences have been shown again to be associated with the spectral content and launching of the initial 2-2-2 pulse into the simulation region. Note also that the above mentioned attenuation is more visible for mode 5, due to its higher cutoff frequency.

## IV. Numerical Experiments

### A. Grating Profile

Two uniform grating profiles, sinusoidal and rectangular, were considered to validate the FDTD simulator. For single

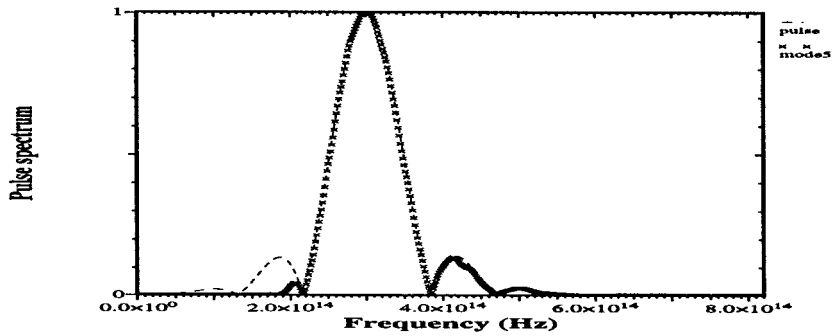


Fig. 4. Spectrum of extracted mode 5.

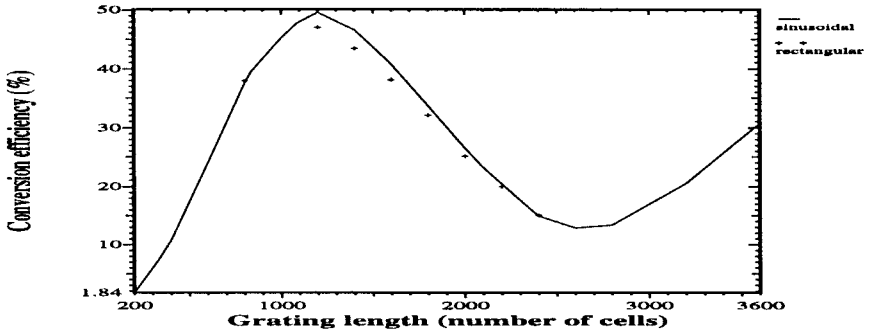


Fig. 5. Comparison of the conversion efficiency achieved by a sinusoidal and a rectangular grating profile.

frequency excitation, coupled-mode theory reveals that the fundamental spatial frequency of the grating controls the mode conversion [2]. This means that both the sinusoidal and rectangular profiles will have the same grating period calculated from the phase matching condition given in (1). Thus, it was expected that the FDTD simulator would predict essentially the same behavior for the fields and the amount of the mode conversion for both of these uniform profiles under single frequency excitation. This was found to be the case. We simulated the propagation of mode 1 at the carrier frequency, $3 \times 10^{14}$ Hz, through a rectangular and a sinusoidal grating. The peak to peak modulation of these profiles was varied, and the maximum mode conversion value was determined numerically. The optimal effective depth was nine cells for the rectangular grating and 12 cells for the sinusoidal grating. These values are very close to the observed ratio of $\pi/4$ reported in [1]. The optimal duty factor of the grating was found to be 1/2.

The gratings are superimposed on the basis waveguide with the grating profile centered in the transverse direction about the core-cladding interface. A grating period of 126 cells ($4.2\lambda_0$) was specified by (1) for the carrier frequency of $3 \times 10^{14}$ Hz. The degree of mode conversion was measured with the FDTD mode extraction technique. We define the conversion efficiency as the ratio of the energy in mode 5 at any location along the guide to the initial energy in mode 1. With these optimized rectangular and sinusoidal profile depths, the FDTD simulator predicted the conversion efficiencies of 90.24 and 94.11%, respectively, from mode 1 to mode 5 in one conversion length. Again, this result was obtained for a single frequency excitation at $3 \times 10^{14}$ Hz; the optimal conversion length for both profiles was 1275 cells (about ten grating periods). The curves showing the amount of conversion versus distance along the waveguide are nearly identical, except for the noted small difference in the peak values. This difference is believed to be due to the differences in the depths of these grating profiles and the FDTD stair-cased approximation used to define the sinusoidal profile.

This mode conversion behavior versus distance along the waveguide persists even in the pulsed mode case. This was somewhat of a surprise since we felt that the smoothness of the sinusoidal profile would make it inherently more broadband. It was tested by exciting the basis waveguide in mode 1 with the 2-2-2 pulse. Fig. 5 shows that the maximum conversion length is about 1200 cells ($40.0\lambda_0$), slightly less than 10 grating periods and slightly less than the single frequency's value. The latter is a result of the polychromatic nature of the 2-2-2 pulse. After the maximum conversion length is reached, mode 5 begins its conversion back into mode 1 (the phase matching condition holds equally as well for converting mode 5 into mode 1). At longer distances the process oscillates between these two conversion processes. These results indicate that a finite grating size (the grating should stop at the maximum conversion length and be followed immediately by the basis waveguide) will provide the optimal conversion length even for a pulsed mode.

### *B. Chirped Grating Designs*

Since the sinusoidal grating provides no distinct advantage over the rectangular grating for the pulsed mode conversion, we had to conceive of other grating schemes to convert

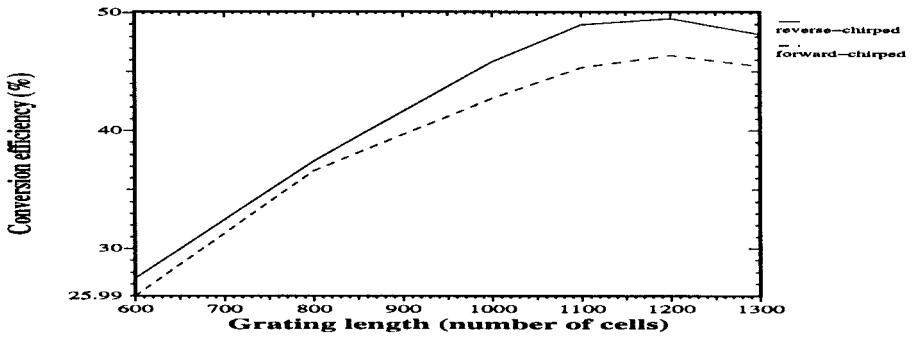


Fig. 6. Mode conversion with linearly chirped gratings.

mode 1 into mode 5 more efficiently. The main issue of mode conversion for a pulsed signal is to design a structure which will efficiently convert major portions of the frequency bandwidth of the excitation signal. Since a grating is inherently a (single frequency) resonant structure, we began the design of a composite structure which consists of several single frequency gratings joined together.

In particular, we designed a linearly reverse-chirped rectangular grating structure. This aperiodic structure is shown in Fig. 2(b). It represents a continuous variation in the unit cell size within the grating. This was accomplished by forming the composite grating from ten corrugations whose periods change linearly from 131 cells to 122 cells. The total length of the structure (1265 cells) is slightly smaller than one conversion length of the uniform grating (1275 cells). The amount of energy converted into mode 5 from the initial mode 1 is shown in Fig. 6. From the figure we observe a slight increase in the conversion efficiency over the uniform rectangular grating. Note that this reverse-chirped grating converts the higher frequency components in the pulse before the lower frequency components. It was also just as easy to test the opposite arrangement. The amount of energy converted into mode 5 from the initial mode 1 by the forward-chirped grating is also shown in Fig. 6. It demonstrates that converting the high frequency components first yields a better overall conversion efficiency over the process which converts the low frequency components first. We have found this to be true in general for any aperiodic grating structure we tested.

### *C. Cascaded Grating Designs*

Similar behavior was observed for a discrete reverse-chirped, cascaded grating structure containing three periods of 131 cells, three periods of 126 cells, and three periods of 121 cells. We decided to pursue this cascaded configuration further since it appears that it would be easier to fabricate than the continuous chirped grating. We found that in both discrete forward- and reverse-chirped gratings, the increase in the overall energy conversion of several of the major frequency components contained in the pulse nicely compensated for the decrease in the energy converted at the carrier frequency due to the smaller conversion length at that frequency. However, it was noticed that more energy at a given frequency would be converted the closer the net length of any one segment of the cascaded grating came to the true conversion length for that frequency.

This design process resulted in a grating structure which had four cascaded rectangular gratings which contained five periods of 133 cells, followed by five periods of 126 cells, five periods of 119 cells, and five periods of 112 cell gratings. These grating periods correspond, respectively, to the frequencies: $3.2 \times 10^{14}$ Hz, $3.0 \times 10^{14}$ Hz, $2.8 \times 10^{14}$ Hz, and $2.5 \times 10^{14}$ Hz. Fig. 7 shows the resulting energy conversion efficiency for the conversion of mode 1 into mode 5 versus the distance in the converter. The designed cascaded reverse-chirped grating achieved an energy conversion efficiency from mode 1 to mode 5 of 60.75%, a 29.45% increase over the 46.93% value for the uniform rectangular grating. This 29.45% improvement is clearly a result of the interactions of multiple frequency components in the signal spectrum with the different grating sections of the composite structure. Notice that the energy in mode 5 continues to build up after passing the distance where the maximum conversion for the uniform grating occurs. The final increase to the 60.75% conversion value is reached approximately at 2200 cells, a 83.33% increase in the length of the grating from its length of 1200 cells in the uniform grating. The maximum energy in mode 5 exists after this much longer conversion length is reached. It takes longer for all of the spectral components to undergo a sufficiently large enough transition for the overall quality of the pulsed mode to be maintained.

The spatial mode pattern of the resulting electric field is given in Fig. 8 for a time after this conversion length has been reached. The corresponding $z$-axis slice is also shown in Fig. 9. Both figures clearly show the presence of mode 1 and mode 5. Furthermore, as expected from their different propagation speeds, mode 1 and mode 5 are well separated in time.

It was also found, as expected, that the individual frequency components contained in the 2-2-2 pulse have different conversion lengths. The lowest frequency component had the largest conversion length; the highest frequency had the shortest conversion length. Since the pulse spectrum contains different amounts of energy at the various frequencies, we decided to design yet another grating structure. An aperiodic cascaded grating was constructed which tailored each segment of the cascade to have a length proportional to the conversion length for its grating period. The resulting grating thus had segments which were designed to convert each frequency component at a closer rate as to the carrier frequency. It had four cascaded rectangular grating segments which contained four periods of

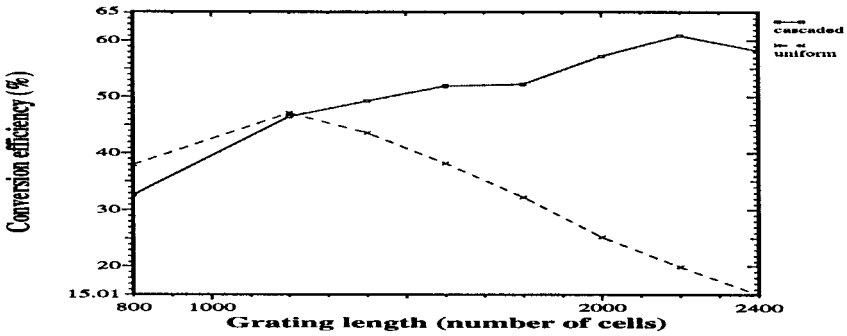


Fig. 7. Energy building-up in mode 5 for the cascaded gratings.

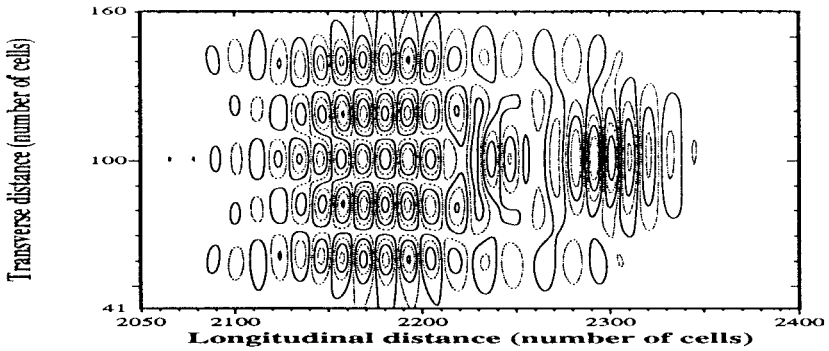


Fig. 8. Field distribution at 5000 time steps.

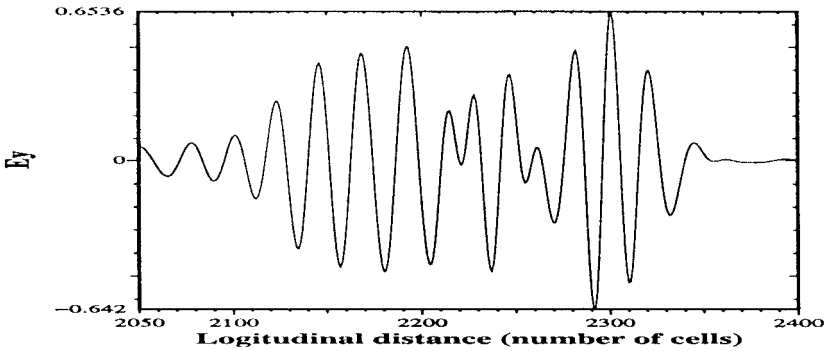


Fig. 9. The $E$ field distribution along the waveguide axis at 5000 time steps.

133 cells, followed by five periods of 126 cells, six periods of 119 cells, and seven periods of 112 cells. We expected a higher efficiency for the overall conversion of the pulsed mode. Unfortunately, this extra design criterion was found to have little effect on the overall efficiency of the pulsed-mode conversion. It was noticed that once a frequency component had been converted, the converted mode 5 deteriorated back to mode 1 the longer it was in contact with the remaining grating structure. Thus while each frequency component was more efficiently converted, the overall improvement became negligible due to the unwanted, continued interactions with the grating structure. We believe that the reason the more uniform numbers of cells provided the best mode conversion was that in addition, the spectrum had proportionately less energy in the frequency components away from the carrier. While, for instance, the lower frequency components needed more conversion length, there was less need to be more efficient at those frequencies since the pulse spectrum contained less energy there.

One final aperiodic grating structure was simulated and is shown in Fig. 2(c). Not only was the grating chirped in frequency, but the depth of the individual segments was also modulated. It was hoped that by varying the depth of the corrugations, the effects of the deterioration of the converted mode due to the increased interaction lengths could be mitigated. In particular the segments of the reverse-chirped grating were designed to be shallower the further along the grating they were found. Thus once a frequency component was converted in one segment of the grating structure, the remaining segments were shallower, thus allowing that higher component to propagate with only minor interactions. We found this depth-modulated reverse-chirped grating did not improve the overall conversion efficiency. Once its depth was varied away from its optimal value, any one segment of the

grating became less efficient. The aperiodic discrete reverse-chirped grating consisting of four segments with five periods in each segment was the most efficient pulsed mode converter.

## V. Conclusion

In this paper, we have presented a numerical simulation approach for investigating the interaction of optical pulses with complex waveguiding geometries. This FDTD method, together with an efficient, real-time mode extraction technique, provides us with a powerful simulation capability to tailor the grating structures to the optical pulses present in the waveguides. The resulting FDTD simulator was used to study and design composite, aperiodic grating structures that were used to convert pulsed modes propagating in dielectric waveguides. An aperiodic discrete, reverse-chirped grating structure was developed which provided a 29.45% improvement in the pulsed mode conversion over that obtainable with a comparable uniform periodic grating.

This FDTD approach is ideal for modeling very complicated waveguiding geometries which involve surface irregularities and complex materials. Detectors based upon mode conversion into cladding modes and waveguide couplers for ultrafast pulsed modes are currently under consideration. Preliminary results with lossy dispersive materials in various grating structures have been obtained and will be reported elsewhere.

## References


[1] R. Petit, *Electromagnetic Theory of Gratings*. New York: Springer-Verlag, 1980.

[2] D. Marcuse, *Theory of Dielectric Optical Waveguides*. New York: Academic, 1991.

[3] A. Yariv, "Coupled-mode theory for guided-wave optics," *IEEE J. Quantum Electron.*, vol. QE-9, pp. 913–933, Sept. 1973.

[4] A. C. Newell and J. V. Moloney, *Nonlinear Optics*. Reading, MA: Addison-Wesley, 1992.

[5] M. D. Feit and J. A. Fleck Jr., "Computation of mode properties in optical fiber waveguides by a propagating beam method," *Appl. Phys.*, vol. 19, no. 7, pp. 1154–1164, 1980.

[6] M. D. Feit and J. A. Fleck Jr., "Mode properties in optical fibers with lossy components by the propagating beam method," *Appl. Phys.*, vol. 20, no. 5, pp. 848–856, 1981.

[7] D. Yevick, W. Bardyszewski, B. Hermansson, and M. Glasner, "Beam propagation methods," in *IEEE Antennas Propagat. Soc. Int. Symp. 1992 Digest: Vol. 1*, New York, IEEE, July 1992, p. 247.

[8] D. Yevick, "A guide to electric field propagation techniques for guided-wave optics," *Optic. Quantum Electron.*, vol. 26, no. 3, pp. 185–97, Mar. 1994.

[9] K. S. Yee, "Numerical solution of initial boundary value problems involving Maxwell's equations in isotropic media," *IEEE Trans. Antennas Propagat.*, vol. AP-44, pp. 302–307, 1966.

[10] A. Taflove, *Computational Electrodynamics*. Norwood, MA: Artech House, 1995.

[11] R. W. Ziolkowski and J. B. Judkins, "Full-wave vector Maxwell equation modeling of the self-focusing of ultrashort optical pulses in a nonlinear Kerr medium exhibiting a finite response time," *J. Opt. Soc. Amer. B*, vol. 10, no. 2, pp. 186–198, 1993.

[12] R. W. Ziolkowski and J. B. Judkins, "Applications of discrete methods to pulse propagation in nonlinear media: Self-focusing and linear-nonlinear interfaces," *Radio Sci.*, vol. 28, no. 5, pp. 901–911, 1993.

[13] R. W. Ziolkowski and J. B. Judkins, "NL-FDTD modeling of linear and nonlinear corrugated waveguides," *J. Opt. Soc. Amer. B*, vol. 11, no. 9, pp. 1565–1575, 1994.

[14] J. B. Judkins and R. W. Ziolkowski, "Finite-difference time-domain modeling of nonperfectly conducting metallic thin-film gratings," *J. Opt. Soc. Amer. A 12*, pp. 1974–1983, 1995.

[15] J. B. Judkins, C. W. Haggans, and R. W. Ziolkowski, "Two-dimensional finite-difference time-domain simulation for rewritable optical disk surface structure design," *Appl. Opt.*, vol. 35, no. 14, pp. 2477–2487, 1996.

[16] J. A. Kong, *Theory of Electromagnetic Waves*. New York: Wiley, 1975.

[17] S. T. Chu and S. K. Chaudhuri, "Combining modal analysis and the finite-difference time domain method in the study of dielectric waveguide problem," *IEEE Trans. Microwave Theory Tech.*, vol. 38, pp. 1755–1760, 1990.

[18] D. G. Dudley, *Mathematical Foundations for Electromagnetic Theory*. Piscataway, NJ: IEEE Press, 1994.



**Tao Liang** received the B.S. degree from Tsing Hua University, Beijing, China, the M.S. degree from Beijing University of Aeronautics and Astronautics, Beijing, China, and the Ph.D. degree from University of Arizona, Tucson, all in electrical engineering in 1986, 1989, and 1997, respectively.

From 1989 to 1993, he worked in the Beijing Institute of Remote Sensing Equipments, Beijing, China, where he performed antenna design, microwave circuit design, and electromagnetic wave propagation analysis. From 1994 to 1997, he was a Research Assistant in the Department of Electrical and Computer Engineering, University of Arizona, where he worked on the electromagnetic modeling of grating assisted devices for microwave and optical applications. Following graduation in July 1997, he joined the Motorola Wireless Infrastructure Systems Division. His research interests include computational electromagnetics, integrated optics, nonlinear microwave device modeling, and electronic packaging design.

**Richard W. Ziolkowski** (M'87–SM'91–F'94) received the Sc.B. degree in physics (magna cum laude) with honors from Brown University, Providence, RI, in 1974, and the M.S. and Ph.D. degrees in physics from the University of Illinois at Urbana-Champaign in 1975 and 1980, respectively.

From 1981 to 1990, he was a member of the Engineering Research Division at the Lawrence Livermore National Laboratory, and from 1984 to 1990, he served as the Leader of the Computational Electronics and Electromagnetics Thrust Area for the Engineering Directorate. In 1990, he joined the Department of Electrical and Computer Engineering at the University of Arizona, Tucson, as an Associate Professor, and in 1996, he was promoted to Full Professor. His research interests include the application of new mathematical and numerical methods to linear and nonlinear problems dealing with the interaction of acoustic and electromagnetic waves with realistic materials and structures.

Dr. Ziolkowski is a member of Tau Beta Pi, Sigma Xi, Phi Kappa Phi, the American Physical Society, the Optical Society of America, the Acoustical Society of America, and Commission B (Fields and Waves) of URSI (International Union of Radio Science). He is an Associate Editor for the IEEE Transactions on Antennas and Propagation. He served as the Vice Chairman of the 1989 IEEE/Antennas and Propagation Society (AP-S) and URSI Symposium in San Jose, CA. For the United States URSI Commission B, he was the Secretary from 1993 to 1996 and is currently serving as the Chairman of Technical Activities Committee. He received the Tau Beta Pi Professor of the Year Award and the IEEE and Eta Kappa Nu Outstanding Teaching Award in 1993.